Geometrically Motivated Inverse Kinematics for an Arm with 7 Degrees of Freedom

Richard Tatum[1] and Drew Lucas [1] and Josh Weaver[1] and Jim Perkins[1]

I. ABSTRACT

The need for robust teleoperated robotic arms is increasing with respect to particular dangerous maritime missions. These missions might include deactivation of underwater mines, underwater salvage, or pipeline repair. In the past, robotic arms with low degrees of freedom were not always feasible for such operations, as the lack of free motion prevented their uses in locations with small space for maneuverability. With higher degrees of freedom, the arms are able to maneuver in tighter spaces and avoid obstacles as well. The increase in the number of degrees of freedom incurs an increase in the computational complexity for determining arm poses. With respect to the 7 degrees of freedom (DOF) Schunk arm, we make observations that allow for the derivation of systems of equations to solve the inverse kinematics problem. Furthermore, we show how to solve the systems such that closed form solutions can be obtained. This approach allows us to give and prove a characterization of the number of solutions with respect to certain conditions. As a surrogate test platform for maritime missions, we have developed a simulation that uses the Robot Operating System (ROS) and ROS visualization (rviz) to simulate the moving of the arm.

II. INTRODUCTION

Maritime missions such as deactivation of underwater mines, underwater salvage, or pipeline repair present their own unique challenges that can represent considerable danger for the human participants. As humans spend more time in hazardous environments, especially when explosives are involved, the likelihood of a catastrophic event increases. To avoid this, we resort to robotic intermediaries which are more expendable than human life and perhaps more suited for very challenging environments. One such intermediary, which is the robotic arm, could be teleoperated in harsh, hostile, maritime environments. To support teleoperation of the robotic arms, the desired goals of the human, namely the position and orientation of the end effector must be mathematically translated into meaningful goals for the arm. Thus, for a given position and orientation of the end effector, we would like to know the value of the joint angles of the arm that place the end effector to achieve the correct position and orientation values. In general, this is the typical inverse kinematic problem that is to be solved for robotic manipulators.

In this paper, we consider a 7 DOF Schunk arm and derive an inverse kinematic solution which is motivated by simple geometric observations. The Schunk 7DOF arm contains 7 revolute joints whose joints are oriented such that the axis of rotation of each joint is orthogonal to the previous joint. Given a desired position T' and orientation D', it is necessary to know how the arm can be positioned so that the end-effector points to T' with the correct orientation D'. Ignoring joint limits and collision detection/avoidance, we have developed a method to provide closed-form solutions for the problem as stated. The seventh joint is radially symmetric and as no other joint is affected by its motion, this joint is fixed to be some arbitrary value. Identification of sections with rotationally invariant lengths yield vectors that must be positioned so that the end-effector can be matched to the proper position and orientation. This analysis yields four distinct vectors, with the middle two being capable of spherical motion. Furthermore, the middle two sections give rise to a free parameter that allows the elbow or fourth joint to be positioned arbitrarily with respect to the end-effector. We show that once these vectors are aligned, we can determine all solutions by recursively solving a system of equations generated by the rotations of the joints.

Our work is most similar to the works of [1], [2]. Korein, perhaps the earliest to study the inverse kinematics of anthropomorphic arms [1], provides a geometric analysis for solutions with joint limits based upon the observation that the elbow can move through a planar circle while the wrist joint is fixed. In [1], the more general kinematic solutions are numerical due to the complexity of the arm. However, for simpler arms, Korein uses the elbow joint and its possible positions to develop an algorithm to determine the joint angles of the arm. We make a similar observation and treat the position of the elbow joint as a free parameter as found in [3]. By identification of sections with rotationally invariant lengths, we derive a set of three spherical equations that can be solved recursively to obtain values for the first six joint angles. Furthermore, through the application of an appropriate transformation, we reduce the left hand side of each equation to the same form that allows for the solutions of each pair of successive joint angles to also be written in the same closed-form. Lee and Ziegler also perform a geometric analysis of a 6R PUMA arm in which the first three joints are computed and used to solve for the remaining three joints

[1]The authors are autonomy researchers associated with Naval Surface Warfare Center Panama City Division, Panama City, FL richard.d.tatum@navy.mil

[2].

Other approaches to this problem exist as well. Closed-loop inverse kinematics have been used in [4] and later in [5] to help guide the motion of a platoon of autonomous vehicles. A gradient-based optimization approach to the inverse kinematics problem was developed in [6]. Wang and Verriest provided a geometric inverse kinematic solution that uses results from minimization of the norm of joint angular velocities [7]. In [8], an iterative inverse kinematics solver was developed that allows for additional arbitrary constraints, and provides a way to resolve conflicting constraints. Genetic algorithms have been developed and used to provide solutions to the inverse kinematics problem as well [9], [10]. In [11], a machine-learning algorithm using relevant training data was implemented to find a solution. While all of these approaches have merit, our approach to the Schunk 7DOF arm provides a closed-form solution that is intuitively clear. As such, we do not require iterative techniques that perform SVD calculations, Jacobian approximations or root estimation of high degree polynomials, which are usually required by many approaches and their associated nonlinear solvers.

The remainder of the paper is organized as follows. Section III gives details describing our approach. Section IV gives an example in which a simulation of the Schunk 7DOF arm is used to demonstrate the validity of our solution. We conclude with a summary given in Section V.

III. Approach

We begin by describing the mathematical framework capable of describing all possible poses of the arm. We denote the ith joint of the arm as $\mathscr{J}_i$, where $1 \leq i \leq 7$. For each joint, we denote the corresponding frame of reference, $\mathscr{F}_i$, which consists of a set of three orthonormal vectors and origin. Associated with each frame of reference is a transformation given by

$$T_1(\theta_1)[v] = R_z(\theta_1) \cdot v + b_0 \quad (1)$$
$$T_2(\theta_2)[v] = R_x(\pi/2)R_z(\theta_2) \cdot v + b_1 \quad (2)$$
$$T_3(\theta_3)[v] = R_x(-\pi/2)R_z(\theta_3) \cdot v + b_2 \quad (3)$$
$$T_4(\theta_4)[v] = R_x(\pi/2)R_z(\theta_4) \cdot v + b_3 \quad (4)$$
$$T_5(\theta_5)[v] = R_x(-\pi/2)R_z(\theta_5) \cdot v + b_4 \quad (5)$$
$$T_6(\theta_6)[v] = R_x(\pi/2)R_z(\theta_6) \cdot v + b_5 \quad (6)$$
$$T_7(\theta_7)[v] = R_x(-\pi/2)R_z(\theta_7) \cdot v + b_6 \quad (7)$$

where R_x and R_z are rotation matrices about the $x-$axis and $z-$axis, respectively, and b_i is the relative origin of the $i-$th frame with respect to the previous frame. See Figure (1a). These transformations will transform vectors from $\mathscr{F}_i$ to $\mathscr{F}_{i-1}$. For each $\mathscr{J}_i$, observe that angle measure of rotation is given by θ_i. For the remainder of the discussion, we will denote vectors that are relative to the global $\mathscr{F}_0$ with the use of the prime symbol, denoted as $'$.

Definition 3.1: Let L_j be a vector that represents a section of the arm whose length is invariant with respect to any rotation of any joint.

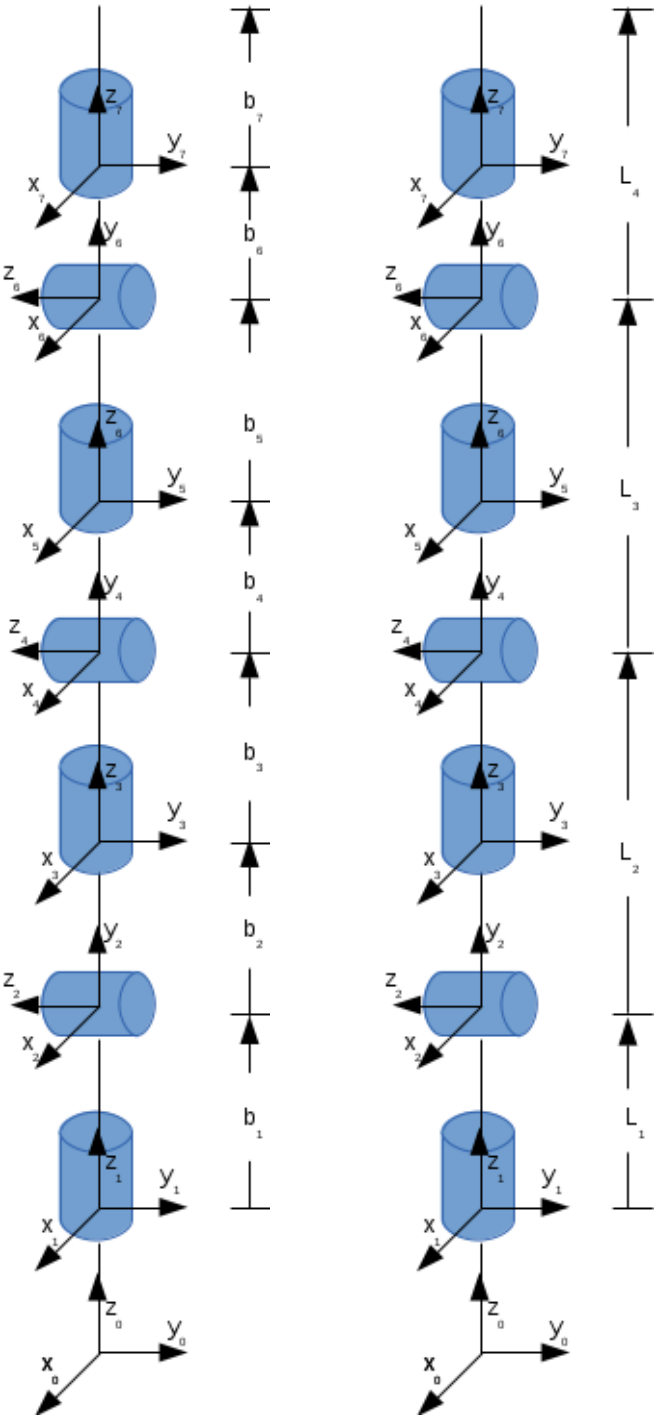

(a) Frames. (b) Invariant Links.

Fig. 1: Schunk 7DOF arm.

With Definition (3.1), we can write

$$L_1 = b_1, \tag{8}$$
$$L_2 = b_2 + b_3, \tag{9}$$
$$L_3 = b_4 + b_5, \tag{10}$$
$$L_4 = b_6 + b_7. \tag{11}$$

Figure (1b) shows the invariant sections identified and we can make some helpful observations. Any possible positioning of the arm will necessarily contain all four links connected in some configuration. If we know all of the link vectors L_1', L_2', L_3' and L_4', then we can easily work backwards to determine θ_i for each joint $\mathscr{J}_i$ required to attain such a configuration. Given that b_0 remains constant and actions of $\mathscr{J}_1$ do not affect b_1, we see that L_1 will also remain constant, allowing for

$$L_1' = L_1. \tag{12}$$

Given that we want the end-effector to achieve a particular orientation and position, L_4' is also determined and is written as

$$L_4' = b_6 \cdot \frac{D'}{\|D'\|}. \tag{13}$$

In fact, Figure (2) shows that if we know where L_2' and L_3' intersect, then all vectors, L_1', L_2', L_3', and L_4', are determined. As L_2' and L_3' are capable of spherical motion, the intersection of L_2' and L_3' occurs along a circle. The location along the circle is a free parameter and shares the same position as the elbow of the arm, which is located at joint $\mathscr{J}_4$. We define the vectors X', R', and P' as

$$L_2' = X' + R', \tag{14}$$
$$P' = L_2' + L_3', \tag{15}$$

where R' has the shortest length from P' to the intersection of L_2' and L_3', and X' points to the location along P' from which R' emanates. Simple calculations show

$$\|X'\| = \frac{\|P'\|^2 + \|L_2'\|^2 - \|L_3'\|^2}{2\|P'\|}, \tag{16}$$
$$\|R'\|^2 = \|L_2'\|^2 - \left(\frac{\|P'\|^2 + \|L_2'\|^2 - \|L_3'\|^2}{2\|P'\|}\right)^2. \tag{17}$$

Furthermore, R' must be orthogonal to P'. Therefore, we are free to choose R such that

$$\langle R', P' \rangle = 0, \tag{18}$$

and with this choice, all links are determined.

We now determine how to rotate the arm from its home position to the desired position given by the configuration of the links. This a matter of simply knowing how to rotate the joints in such a way that the following equations are satisfied:

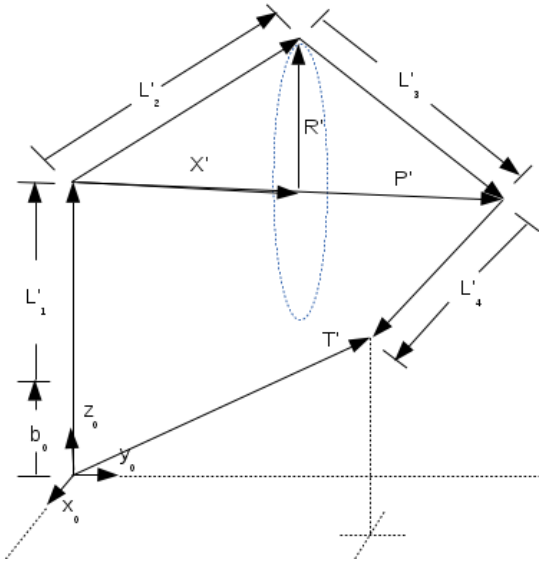

Fig. 2: Given a target T' and orientation vector that coincides with L_4', we can construct several poses that solve this problem. The blue circle with radius vector R' denotes all potential intersections of L_2' and L_3' and indicates potential new configurations and solutions.

$$b_1' = \|b_1\| \frac{L_1'}{\|L_1'\|} \tag{19}$$
$$b_2' = \|b_2\| \frac{L_2'}{\|L_2'\|} \tag{20}$$
$$b_3' = \|b_3\| \frac{L_2'}{\|L_2'\|} \tag{21}$$
$$b_4' = \|b_4\| \frac{L_3'}{\|L_3'\|} \tag{22}$$
$$b_5' = \|b_5\| \frac{L_3'}{\|L_3'\|} \tag{23}$$
$$b_6' = \|b_6\| \frac{L_4'}{\|L_4'\|} \tag{24}$$
$$b_7' = \|b_7\| \frac{L_4'}{\|L_4'\|} \tag{25}$$

Examination of the arm reveals that the pair of joints $(\mathscr{J}_1, \mathscr{J}_2)$ are equivalent to joint pairs $(\mathscr{J}_3, \mathscr{J}_4)$ and $(\mathscr{J}_5, \mathscr{J}_6)$ with respect to the types of achievable motion. Clearly, pairs $(\mathscr{J}_1, \mathscr{J}_2)$, $(\mathscr{J}_3, \mathscr{J}_4)$, and $(\mathscr{J}_5, \mathscr{J}_6)$ must be rotated to satisfy

$$T_1 T_2 b_2 = \sum_{k=0}^{2} b_k', \tag{26}$$
$$T_1 T_2 T_3 T_4 b_4 = \sum_{k=0}^{4} b_k', \tag{27}$$
$$T_1 T_2 T_3 T_4 T_5 T_6 b_6 = \sum_{k=0}^{6} b_k', \tag{28}$$

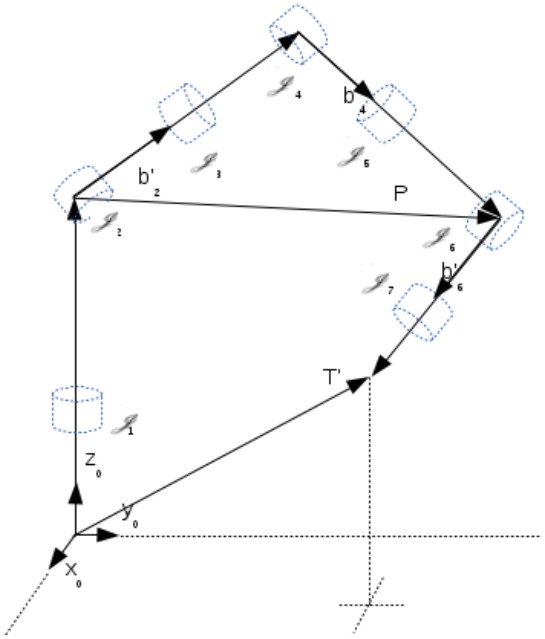

Fig. 3: With links L'_1, L'_2, L'_3, and L'_4 specified as in Figure (2), we can determine the angles needed to rotate the joints to achieve such a configuration.

where we have momentarily dropped the dependence upon θ_i for ease of exposition. Rewriting these equations, we have

$$T_1T_2b_2 = \sum_{k=0}^{2} b'_k, \tag{29}$$

$$T_3T_4b_4 = T_2^{-1}T_1^{-1}\sum_{k=0}^{4} b'_k, \tag{30}$$

$$T_5T_6b_6 = T_4^{-1}T_3^{-1}T_2^{-1}T_1^{-1}\sum_{k=0}^{6} b'_k. \tag{31}$$

Let S_1 and S_2 be as

$$S_1(0)[v] = T_1(0)[v] \tag{32}$$
$$S_3(0)[v] = T_3(0)[v] \tag{33}$$
$$S_5(0)[v] = T_5(0)[v] \tag{34}$$
$$\tag{35}$$

then we can apply these transformations as follows

$$S_1^{-1}T_1T_2b_2 = d_1, \tag{36}$$
$$S_3^{-1}T_3T_4b_4 = d_2, \tag{37}$$
$$S_5^{-1}T_5T_6b_6 = d_3. \tag{38}$$

where

$$d_1 = S_1^{-1}\sum_{k=0}^{2} b'_k \tag{39}$$

$$d_2 = S_3^{-1}T_2^{-1}T_1^{-1}\sum_{k=0}^{4} b'_k \tag{40}$$

$$d_3 = S_5^{-1}T_4^{-1}T_3^{-1}T_2^{-1}T_1^{-1}\sum_{k=0}^{6} b'_k. \tag{41}$$

Observe that the left hand side of Equations (36) - (38) have exactly the same form. We now give a condition characterizing the existence of solutions.

Proposition 3.1: For the Schunk 7DOF arm, let L'_j be as defined by Definition (3.1) and shown in Figure (3), and consider the transformations T_i as given by (1) - (7). For X', R', and P' as given by (14) - (15), if

$$\frac{\|P'\|^2 + \|L'_2\|^2 - \|L'_3\|^2}{2\|P'\|} > \|L'_2\|,$$

there are no solutions. If

$$0 \leq \frac{\|P'\|^2 + \|L'_2\|^2 - \|L'_3\|^2}{2\|P'\|} \leq \|L'_2\|,$$

there are 8 solutions.

Proof: For the first part of this proof, suppose that $\|X'\| > \|L'_2\|$. Since $\|L'_2\|^2 = \|X'\|^2 + \|R'\|^2$, we have $\|L'_2\| = \|X'\|^2 + \|R'\|^2 < \|X'\|$, which implies $\|R'\|^2 < 0$ and no solutions are possible.

If $\|X'\| \leq \|L'_2\|$, then links L'_1, L'_2, L'_3, and L'_4 are connected, which implies that the right hand side of all equations in Equations (36) - (38) exist. Since, $S_1^{-1}T_1T_2b_2 = d_1$, we have

$$\begin{bmatrix} -\cos(\theta_1)\sin(\theta_2) \\ -\sin(\theta_1)\sin(\theta_2) \\ \cos(\theta_2) \end{bmatrix} \|b_2\| + b_1 = d_1, \tag{42}$$

which yields the following solution

$$\theta_1 = \tan^{-1}\left(\frac{d_{1,y}}{d_{1,x}}\right) \tag{43}$$

$$\theta_2 = -\cos^{-1}\left(\frac{d_{1,z} - \|b_1\|}{\|b_2\|}\right). \tag{44}$$

An application of forward solving shows that $T_1T_2b_2 = b'_0 + b'_1 + b'_2$. However, the only other solution for this case is to rotate $\mathscr{J}_1$ by $\theta_1 + \pi$ and $\mathscr{J}_2$ by $-\theta_2$, giving the remaining solution. With the two solutions from (36), we can proceed to solve (37) in the same manner. Of course, for each solution of (36), we get two solutions for (37). Continuing to (38), we see that we will have a total of 8 solutions. As $\mathscr{J}_7$ has only one degree of freedom, it only has one solution and does not increase the number of solutions. ■

Proposition (3.1) contains the algorithm for determining the solutions for the arm. Simply stated, solve (36) to get values for θ_1 and θ_2. With these solutions, recursively proceed by

TABLE I: All of the solutions for a fixed elbow joint that place the end-effector at the correct position and orientation.

$\mathscr{J}_1$	$\mathscr{J}_2$	$\mathscr{J}_3$	$\mathscr{J}_4$	$\mathscr{J}_5$	$\mathscr{J}_6$
θ_1	θ_2	θ_3	θ_4	θ_5	θ_6
θ_1	θ_2	θ_3	θ_4	$-\theta_5$	$\theta_6 + \pi$
θ_1	θ_2	$-\theta_3$	$\theta_4 + \pi$	θ_5	θ_6
θ_1	θ_2	$-\theta_3$	$\theta_4 + \pi$	$-\theta_5$	$\theta_6 + \pi$
$-\theta_1$	$\theta_2 + \pi$	θ_3	θ_4	θ_5	θ_6
$-\theta_1$	$\theta_2 + \pi$	θ_3	θ_4	$-\theta_5$	$\theta_6 + \pi$
$-\theta_1$	$\theta_2 + \pi$	$-\theta_3$	$\theta_4 + \pi$	θ_5	θ_6
$-\theta_1$	$\theta_2 + \pi$	$-\theta_3$	$\theta_4 + \pi$	$-\theta_5$	$\theta_6 + \pi$

solving the next system, until we are done. The solutions for the angles are given as

$$\theta_3 = \tan^{-1}\left(\frac{d_{2,y}}{d_{2,x}}\right), \tag{45}$$

$$\theta_4 = -\cos^{-1}\left(\frac{d_{2,z} - \|b_3\|}{\|b_4\|}\right), \tag{46}$$

$$\theta_5 = \tan^{-1}\left(\frac{d_{3,y}}{d_{3,x}}\right), \tag{47}$$

$$\theta_6 = -\cos^{-1}\left(\frac{d_{3,z} - \|b_5\|}{\|b_6\|}\right). \tag{48}$$

Table (I) shows all of the solutions. The next section provides an example using this technique to help validate our approach.

IV. Example

Our algorithm is implemented in C++ and uses ROS and RVIZ to move and display the arm. For this example, we position the base of the robot at $(300, 0, 0)$ and want the hand to be placed at $(900, 0, 908)$, assuming an orientation of $(.864405, 0, .502796)$. The orientation was chosen so that the hand would either point upwards or downwards, depending upon the desired position and the origin of $\mathscr{F}_1$. We select $\theta_7 = 0$ and Figures (4) - (9) show the results.

Note that of the eight solutions for each pose, the solution that was closer to the home position with respect to the Euclidean distance was chosen. Figures (4) and (5) show the arm initially transitioning from the home position. Figures (6) - (9) show that the arm is in the correct position and orientation, but with different orientations of the elbow joint.

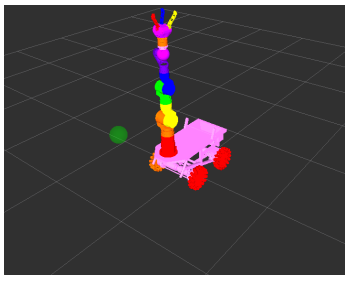

Fig. 4: Home position.

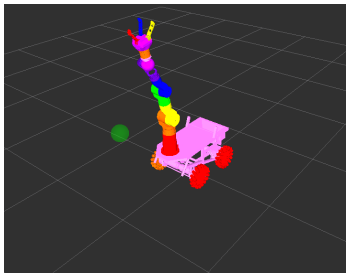

Fig. 5: Transitioning step.

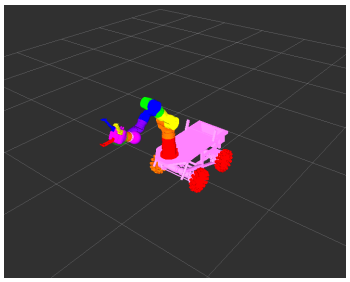

Fig. 6: Elbow pointing up.

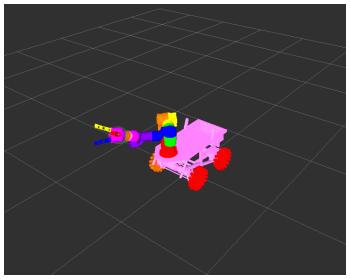

Fig. 7: Elbow pointing right.

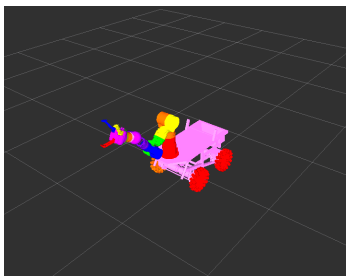

Fig. 8: Elbow pointing down

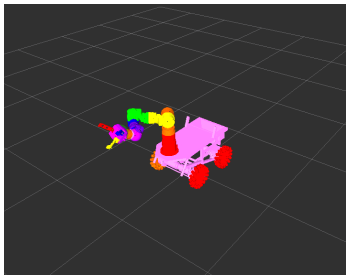

Fig. 9: Elbow pointing right.

V. Summary

We have constructed an approach for positioning the Schunk 7DOF arm into the correct position and orientation.

Furthermore, this approach uses a free parameter that allows for the positioning of the elbow located at the fourth joint. We have also provided a sufficient condition for classifying the number of solutions, based upon the desired position and orientation of the end-effector. This condition serves to perform a priori checks to determine if the desired position and orientation is attainable. A future area of investigation involves general path planning, and specifically, the proper choice of the elbow joint when considering additional constraints such as obstacle avoidance.

REFERENCES

[1] J. Korein, "A geometric investigation of reach," Ph.D. dissertation, University of Pennsylvania, 1985.

[2] C. Lee and M. Ziegler, "Geometric approach in solving inverse kinematics of puma robots," *Aerospace and Elect. Syst.*, vol. AES-20, no. 6, pp. 695–706, 1984.

[3] D. Tolani, A. Goswami, and N. Badler, "Real-time inverse kinematics techniques for anthropomorphic limbs," *Graphical Models*, no. 62, pp. 353–388, 2000.

[4] P. Chiacchio, S. Chiaverini, L. Sciavicco, and B. Siciliano, "Close-loop inverse kinematics schemes for constrained redundant manipulators with task space augmentation and task priority strategy," *International Journal of Robotics Research*, vol. 10, no. 4, pp. 410–425, 1991.

[5] G. Antonelli and S. Chiaverini, "Kinematic control of platoons of autonomous vehicles," *IEEE Transactions on Robotics*, vol. 22, no. 6, 2006.

[6] J. Zhao and N. Badler, "Inverse kinematics positioning using nonlinear programming," *ACM Transactions on Graphics*, vol. 13, no. 4, pp. 313–336, 1994.

[7] X. Wang and J. Verriest, "A geometric algorithm to predict the arm reach posture for computer-aided ergonomic evaluation," *Journal of Visualization and Computer Animation*, vol. 9, no. 1, pp. 33–47, 1998.

[8] P. Baerlocher and R. Boulic, "An inverse kinematic architecture enforcing an arbitrary number of strict priority levels," *Vistual Computer 20*, no. 6, pp. 402–417, 2004.

[9] A. Khwaja, M. Rahman, and M. Wagner, "Inverse kinematics of arbitrary robotic manipulators using genetic algorithms," *Advances in Robotic Kinematics: Analysis and Control*, pp. 375–382, 1998.

[10] P. Kalra, P. Mahapatra, and D. Aggarwal, "An evolutionary approach for solving the multimodal inverse kinematics problem of industrial robots," *Mechanism and Machine Theory*, vol. 41, no. 10, pp. 1213–1229, 2005.

[11] K. Grochow, S. Martin, A. Hertzmann, and Z. Popovic, "Style-based inverse kinematics," *ACM Transactions on Graphics*, vol. 23, no. 3, 2004.